



# The phospha-Michael addition of dimethyl- and diphenylphosphites to the $\eta^1$ -*N*-maleimidato ligand: Inhibition of serine hydrolases by half-sandwich metallocarbonyl azaphosphonates

Bogna Rudolf<sup>a,\*</sup>, Michèle Salmain<sup>b</sup>, Marcin Palusiak<sup>c</sup>, Janusz Zakrzewski<sup>a</sup>

<sup>a</sup> Department of Organic Chemistry, University of Łódź 90-136 Łódź, Narutowicza 68, Poland

<sup>b</sup> Ecole Nationale Supérieure de Chimie de Paris, Laboratoire de Chimie et Biochimie des Complexes Moléculaires (UMR CNRS 7576),

11 rue Pierre et Marie Curie 75231 Paris cedex 05, France

<sup>c</sup> Department of Crystallography, University of Łódź, 90-136 Łódź, Pomorska 149/153, Poland

## ARTICLE INFO

### Article history:

Received 9 September 2008

Received in revised form 24 October 2008

Accepted 27 October 2008

Available online 8 November 2008

### Keywords:

Metallocarbonyl compounds

Bioorganometallic chemistry

Phosphonates

Serine hydrolases

Cholinesterases

## ABSTRACT

Dialkyl- and diphenyl phosphites react with the  $(\eta^5\text{-C}_5\text{H}_5)\text{M}(\text{CO})_x(\eta^1\text{-N-maleimidato})$  ( $\text{M} = \text{Fe}, \text{Mo}; x = 2$  or 3) complexes giving products of the phospha-Michael addition to the  $\eta^1$ -*N*-maleimidato ligand. One of these complexes ( $\text{M} = \text{Fe}, x = 2$ ) was characterized by X-ray diffraction. The synthesized metallocarbonyl azaphosphonates and the corresponding iron phosphonic acid act as inhibitors of certain serine hydrolases (AChE and BChE). The kinetic assays were performed and revealed that inhibition mechanism depends strongly on the enzyme and the structure of the inhibitor.

© 2008 Elsevier B.V. All rights reserved.

## 1. Introduction

Organometallic complexes carrying phosphonato groups (phosphonates or corresponding phosphonic acids) have attracted considerable interest [1] within the last years due in part to their ability to strongly bind to metal oxide solid supports. This feature enables immobilization of organometallic moieties (e.g. redox-active ferrocenyl groups) on robust inorganic backbones, which may be of interest for many branches of materials science [2]. On the other hand, phosphonates having azaheterocyclic substituents may manifest interesting biological activities [3].

We have been interested for a long time in the chemistry of the  $(\eta^5\text{-C}_5\text{H}_5)\text{M}(\text{CO})_x(\eta^1\text{-N-maleimidato})$  complex **1a** [4] and, more recently, in that of its molybdenum and tungsten analogs **1b** and **1c** [5]. The ethylenic bond of the maleimidato ligand in these complexes is readily attacked by nucleophiles such as thiols, amines or imidazoles. These reactions can be used to introduce IR-detectable moieties on peptides and proteins with potential applications in immunoassays [6–10].

In this paper, we describe the addition of dialkyl phosphites to the ethylenic bond in **1a–c** leading to phosphonates bearing metallocarbonyl moieties. The X-ray structural study of phosphonate **2a**

is also disclosed and discussed. The biochemical activity of some of these new phosphonates towards selected serine hydrolases: acetylcholinesterase (AChE) and butyrylcholinesterase (BChE) was investigated. It appeared that the diphenyl phosphonate ester derived of **1a** behaved as a competitive inhibitor of the serine esterase BChE in a short timescale and inactivated this enzyme in a time-dependent fashion by phosphorylation of its active site serine residue.

## 2. Results

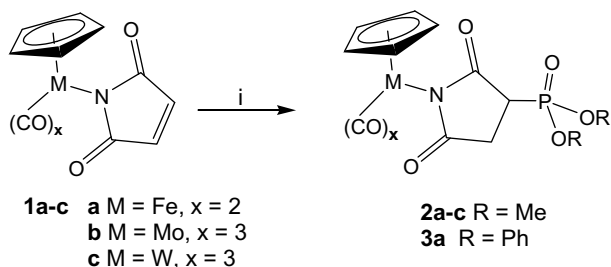
### 2.1. Synthesis of phosphonates **2a–c** and **3a–b**

We found that complexes **1a–c** react in dichloromethane at r.t. with dimethyl- and diphenyl phosphite in the presence of a stoichiometric amount of DBU to afford phosphonates **2a–c** and **3a** as fairly air-stable yellow solids or oils (Scheme 1).

The <sup>1</sup>H NMR spectrum of these compounds did not show ethylenic protons signals characteristic of **1a–c**, but instead complex patterns, assignable to the CH–CH<sub>2</sub> entity, coupled with <sup>31</sup>P were observed at 2.9–3.4 ppm. The <sup>13</sup>C NMR spectrum of **2a** showed coupling of all carbons of the succinimide ring with <sup>31</sup>P, indicating creation of the C–P bond. The <sup>31</sup>P NMR spectra of **2a–c** and **3a** displayed a singlet in the region between 10 and 25 ppm characteristic for phosphonates. Their IR spectra apart from two

\* Corresponding author. Tel.: +48 42 6355755.

E-mail address: [brudolf@chemul.uni.lodz.pl](mailto:brudolf@chemul.uni.lodz.pl) (B. Rudolf).



**Scheme 1.** Conditions: (i)  $\text{HP}(=\text{O})(\text{OR})_2$ , DBU in  $\text{CH}_2\text{Cl}_2$ .

metallocarbonyl stretching bands  $\sim 2000\text{ cm}^{-1}$  and an imide carbonyl stretching band  $\sim 1650\text{ cm}^{-1}$  displayed a strong absorption band around  $1200\text{ cm}^{-1}$ , assignable to the stretching vibration of the P=O bond.

## 2.2. X-ray structure of **2a**

The crystallographic data and selected geometrical parameters of **2a** are collected in Tables 1 and 2 respectively. Compound **2a** crystallized in monoclinic  $P2_1/c$  space group with one molecule per asymmetric unit cell. The central iron atom was four-coordinated and the whole complex adopted the so-called “piano-stool” structure which seems to be characteristic for this type of coordination environment (Fig. 1). The distance between the central atom and the centroid of the Cp ring was  $1.724(3)\text{ \AA}$ , i.e. very close to the distance between the central atom and the best plane of this ring for which a distance of  $1.723(4)\text{ \AA}$  was measured. This arises from the relatively similar distances between the iron and carbon atoms forming Cp ring; the range is  $2.066(5)$ – $2.100(4)\text{ \AA}$  with a maximum for C1, with a mean value of  $2.082(15)\text{ \AA}$ . The best plane of Cp ring formed an angle of  $33.1(2)^\circ$  with the best plane of the ring of succinimidato ligand. It is worth mentioning that the succinimidato ligand was partially twisted along the Fe–N bond. The value of the torsion angle formed by Fe, N8, C10 and C11 atoms is  $177.8(1)^\circ$ , which means that the succinimidato ligand was twisted along the coordinating bond by more than  $2^\circ$ . As a result, the angle between the Cp centroid, Fe and the succinimidato ring centroid was equal to  $121.3(1)^\circ$  instead of value close to  $146^\circ$  ( $180^\circ - 33.1^\circ$  gives  $145.9^\circ$ ). Interestingly, the dimethyl phosphonate group was attached to the succinimidato ligand in the direc-

**Table 1**  
Crystallographic data and structure refinement of **2a**.

Formula	$\text{C}_{13}\text{H}_{14}\text{FeNO}_7\text{P}$
Formula weight	383.07
Crystal system	Monoclinic
Space group	$P2_1/c$
<i>a</i> (Å)	10.784(13)
<i>b</i> (Å)	12.551(10)
<i>c</i> (Å)	12.533(6)
$\beta$ ( $^\circ$ )	111.43(5)
<i>V</i> (Å <sup>3</sup> )	1579(2)
<i>Z</i>	4
<i>D</i> <sub>calc</sub> (g/cm <sup>3</sup> )	1.611
Crystal size (mm)	0.11 × 0.14 × 0.16
Temperature (K)	293
Radiation (Å)	Mo $K\alpha$ , 0.71069
$\theta$ Minimum–maximum ( $^\circ$ )	2.0–27.5
Dataset <i>h</i> ; <i>k</i> ; <i>l</i>	0:14; 0:16; –16:15
Total/unique data/ <i>R</i> <sub>int</sub>	3815/3629/0.037
Observed data [ <i>I</i> > 2.0 $\sigma$ ( <i>I</i> )]	2557
Number of reflections	3629
Number of parameters	210
<i>R</i> , <i>wR</i> <sup>2</sup> , <i>S</i>	0.0326, 0.1104, 0.98
Minimum/maximum residual density (e Å <sup>−3</sup> )	−0.35/0.43

**Table 2**  
Selected geometrical parameters of **2a** (Å,  $^\circ$ ).

Fe–C6	1.786(3)
Fe–C7	1.790(3)
Fe–N8	1.975(2)
O9–C9	1.219(3)
O12–C12	1.210(3)
P10–C10	1.804(3)
P10–O20	1.458(3)
P10–O21	1.573(2)
P10–O22	1.568(2)
O2–P10–O21	102.69(11)
O20–P10–C10	113.76(13)
O12–C12–N8	125.3(2)
O12–C12–C11	124.6(2)
O7–C7–Fe	175.6(3)
O6–C6–Fe	179.1(3)
C6–Fe–C7	93.62(15)
Fe–N8–C9–C10	−178.72(15)
N8–C9–C10–P10	−122.95(19)
O20–P10–C10–C9	52.9(2)
C10–P10–O21–C21	104.6(2)
C10–P10–O22–C22	−175.5(2)

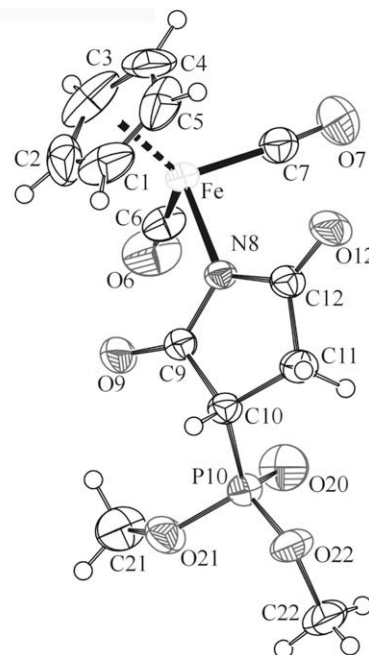
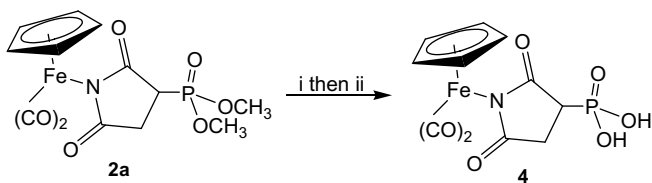


**Fig. 1.** Molecular structure of **2a**. Thermal ellipsoids were drawn with 30% probability.

tion opposite to the Cp ring. As the result, the P10–O20 vector formed a torsion angle of  $163.7(5)^\circ$  with the vector running between Fe center and the centroid of the Cp ring. There was a lack of typical hydrogen bonds that could stabilize the crystal structure, since there is a lack of typical proton donating groups. The only intermolecular interaction, which can additionally stabilize the crystal packing, seems to be a  $\text{P}=\text{O} \cdots \text{C}\equiv\text{O}$  interaction [11] formed by P10–O20 and C6–O6 bonds. The  $\text{O}20 \cdots \text{C}6^i$  (symmetry code *i*:  $2 - x, -1/2 + y, 3/2 - z$ ) distance equals  $3.064(5)\text{ \AA}$ .

## 2.3. Synthesis of phosphonic acid **4**

Transesterification of **2a** with TMSBr followed by reaction with methanol afforded the metallocarbonyl phosphonic acid **4** (Scheme 2). The compound was soluble in water and methanol and insolu-



**Scheme 2.** Conditions: (i) TMSBr, CH<sub>2</sub>Cl<sub>2</sub> and (ii) MeOH.

ble in other organic solvents. The <sup>1</sup>H NMR spectrum of **4** lacked the two methyl protons doublets characteristic of **2a**. The <sup>31</sup>P signal shifted downfield to 15.86 ppm. The same reaction attempted with **3a** failed, leaving substrate **3a** unchanged.

## 2.4. Biochemical studies

### 2.4.1. Reversible inhibition experiments

It has been shown recently that simple dialkyl phenyl phosphates were able to inhibit AChE and/or BChE in a reversible manner by a competitive or partially competitive mechanism [12]. Earlier, Casida and coll. showed that several phosphonic acids derived from the agrochemical ethephon were competitive inhibitors of BChE [13]. We thought it interesting to examine whether complexes **2a** and **3a** together with phosphonic acid **4** were also able to inhibit AChE and BChE and what the inhibition mechanism may be. In a typical experiment, enzyme was mixed with complex at a fixed concentration and substrate at various concentrations and the enzyme activity of the samples was measured accordingly. Initial hydrolysis rates were plotted versus substrate concentration and non linear regression analysis of the data yielded the dissociation constants gathered in Table 3.

It was immediately observed that **2a** (at a concentration up to 1.8 mM) had no effect on the activity of AChE and BChE, indicating that this compound was not able to bind to any of these enzymes. The phosphonic acid derivative **4** was shown to behave as a mixed-type inhibitor for both AChE and BChE, indicating that this

**Table 3**  
Dissociation constants  $K_i$  and  $K'_i$  for the inhibition of AChE and BChE by complexes **2a**, **3a** and **4**.

Complex	Enzyme	Type of inhibition	Inhibition constants
<b>2a</b>	AChE	No inhibition	–
	BChE	No inhibition	–
<b>3a</b>	AChE	No inhibition	–
	BChE	Competitive	$K_i = 0.14$ mM
<b>4</b>	AChE	Mixed	$K_i = 0.6$ mM $K'_i = 2.4$ mM
	BChE	Mixed	$K_i = 0.9$ mM $K'_i = 1.7$ mM

compound was able to bind to both free enzymes and enzyme–substrate complexes with different dissociation constants  $K_i$  and  $K'_i$ . Finally, **3a** behaved as a competitive inhibitor towards BChE (this experiment was made possible because irreversible inhibition occurs very slowly, see below), whereas it had no effect on AChE.

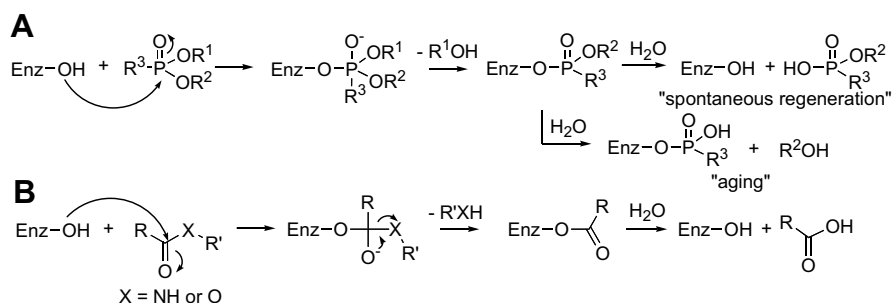
### 2.4.2. Irreversible inhibition experiments

Organophosphorus (OP) compounds of various structures (phosphonates, phosphates, phosphofluoridates, phosphoramidates) have long been known as irreversible inhibitors of serine hydrolases (esterases, lipases, proteases) [14–16]. The mechanism by which these compounds inhibit these enzymes is well established. It consists in the phosphorylation of the active site serine residue in a similar manner as the substrate temporarily acylates the same site (Scheme 3).

In this line, several OP chemicals have been employed as chemical warfare agents (“nerve agents”). Others are broadly used in agriculture as insecticides. Only two compounds belonging to this family are actually used as pharmaceuticals, namely echothiophate for glaucoma treatment and metrifonate for the chemotherapy of schistosomes [17]. In all these cases, the mechanism of action of the OP compounds involved the irreversible inhibition of AChE.

In the same line, several diesters of simple phosphonic acids of the general formula alkyl-P(=O)(OEt)(OC<sub>6</sub>H<sub>4</sub>-pNO<sub>2</sub>) are potent irreversible inhibitors of AChE with IC<sub>50</sub> values of ca. 0.1 μM. These compounds inhibit to a lesser extent the serine protease chymotrypsin (CT) with IC<sub>50</sub> ranging from 1 μM to 1 mM depending of the alkyl chain length [18]. Other phosphonates containing a *p*-nitrophenyl group were also shown to irreversibly inhibit trypsin, CT and BChE [19,20]. More recently, van Koten and coll. reported the synthesis of a phosphonate derivative carrying an organometallic pincer complex that site-selectively labeled the active site serine of the lipase cutinase [21]. Diphenyl phosphonate esters with a peptidic substituent were shown as irreversible inhibitors of certain serine proteases [22].

Therefore, we thought it interesting to investigate whether the new phosphonate diester complexes **2a** and **3a** were also able to inactivate the serine hydrolases AChE, BChE and CT in a time-dependent manner. In a typical experiment, enzyme was incubated with complex in large excess. Aliquots were removed from time to time and the enzyme activity of the mixtures measured with appropriate substrates. No loss of activity was observed for the mixtures of AChE and either **2a** or **3a** compared to control, indicating that none of these phosphonate diesters were able to inactivate the enzyme. Conversely, gradual loss of enzymatic activity of the mixtures of BChE and **2a**, BChE and **3a** and CT and **3a** was noticed. For the two mixtures containing **3a**, the % remaining activity plotted as a function of time followed as expected a first order law from which was deduced the  $k_{obs}/[I]$  ( $k_{obs}$  is the pseudo-first order rate constant; I is **3a**) of  $8.6 \pm 0.4$  M<sup>-1</sup> min<sup>-1</sup> for BChE and  $0.66 \pm 0.04$  M<sup>-1</sup> min<sup>-1</sup> for CT (Fig. 2).



**Scheme 3.** (A) Mechanism of inhibition of serine hydrolases by OP compounds. (B) Simplified mechanism of hydrolysis catalyzed by serine hydrolases.

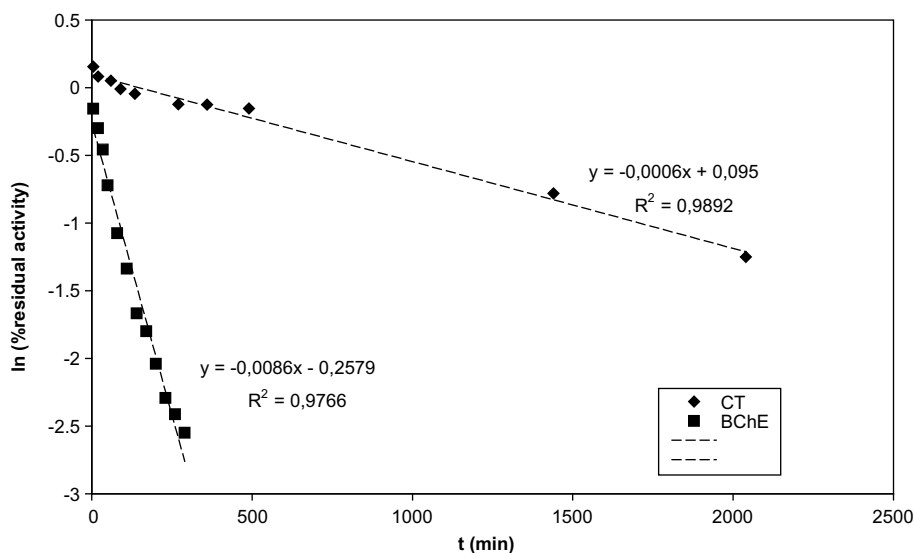


Fig. 2. Time-dependent inactivation of BChE and CT by **3a** at 1 mM.

In the case of the BChE and **2a**, the gradual decrease of enzymatic activity did not obey a first order kinetics law (results not shown). In fact, it was observed the gradual appearance of a precipitate that may have been responsible for the loss of activity. Indeed resuspension of the precipitate completely restored the enzymatic activity of the mixture as compared to control experiment.

Further experiments were then carried out with **3a** and BChE. First, the ability to inhibit BChE was also evidenced by measuring the  $IC_{50}$  after incubation for 60 min, i.e. the concentration of complex that decreases by 50% the enzyme activity. It was equal to 220  $\mu$ M. Second, experiments were also carried out to shed a light on the mechanism of inhibition of BChE. If **3a** inactivates BChE via the mechanism depicted in Scheme 3, it is likely that the enzyme can be reactivated via dephosphonylation, either spontaneously [23] or by addition of a reactivator such as the oxime pralidoxime [24]. Therefore, an enzyme sample incubated overnight with **3a** was first submitted to gel filtration so as to remove excess complex. The enzymatic activity of the purified protein was low (1.8% with respect to control sample), indicating that inhibition by **3a** was indeed irreversible in the short term. Then one half of the protein solution was allowed to stand at room temperature while pralidoxime was added to the other half (final concentration 2 mM). The % reactivation measured after 15 and 24 h are reported as a bar chart (Fig. 3).

Very slow reactivation of enzyme towards BTCh hydrolysis was observed with time. Pralidoxime noticeably accelerated enzyme reactivation. It is interesting to note that only 15% of enzymatic activity was spontaneously recovered for the modified BChE after 10 days, so that the simultaneous dealkylation process, i.e. the so-called aging process, yielding a permanently inhibited enzyme (see Scheme 3) may have occurred concurrently.

Eventually, the sample of BChE treated overnight with **3a** and submitted to gel filtration was analyzed by IR spectroscopy. In the 1800–2200  $cm^{-1}$  spectra range, the spectrum displayed two weak but clearly detectable bands at 2054 and 1983  $cm^{-1}$ , the latter one being weaker than the former (Fig. 4, upper trace). For comparison, the IR spectrum of **3a** was recorded in the same conditions (Fig. 4, lower trace). As expected, compound **3a** gave two  $\nu$ CO bands at 2054 and 2006  $cm^{-1}$  characteristic of the symmetric and asymmetric stretching vibration modes of the two CO ligands. It indicated that the metallocarbonyl complex was indeed covalently bound to the protein. Furthermore, the protein environment in which the complex was embedded affected the vibration of the

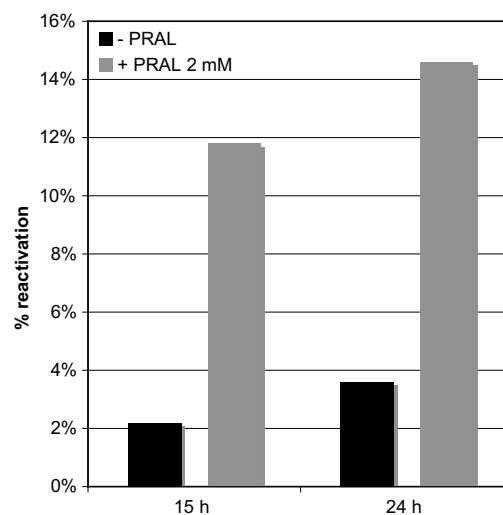


Fig. 3. Time-dependent reactivation of BChE inhibited by **3a**. Inhibited BChE was incubated in Tris–HCl pH 7.6 as is or in the presence of 2 mM pralidoxime.

CO ligands. Why it only changed the asymmetric vibration mode remains unclear.

This set of experiments gave a good indication that **3a** inhibited BChE by phosphonylation of its active site serine residue (Ser 196 in horse serum BChE). The inhibited enzyme undergoes a very slow dephosphonylation process leading to partial activity recovery. This process is accelerated by addition of pralidoxime.

### 3. Discussion

Addition of dialkyl phosphates to electron-poor ethylenic bonds (phospha-Michael reaction) has been widely studied in the field of organic compounds [25]. For example, Tan and coll. have studied this reaction using maleimides as Michael acceptors [26]. As part of our earlier work, we showed that the reaction between thiols and the maleimidato ligand in complexes **1a–c** did occur but its rate was significantly slower compared to that with *N*-ethylmaleimide. In this work, we show that addition of dialkylphosphites to a

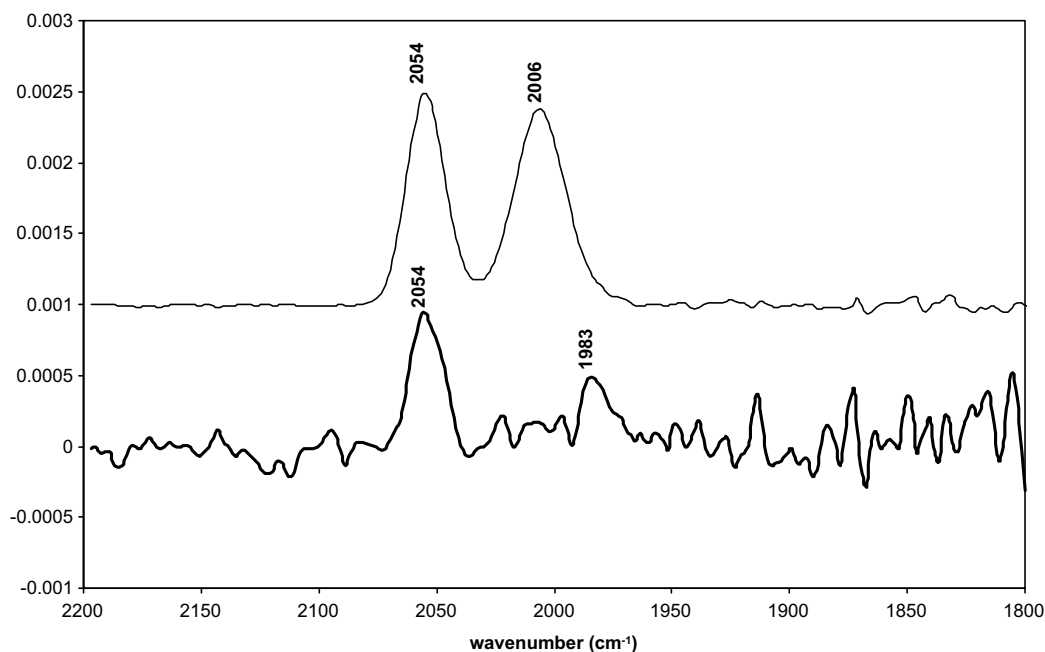


Fig. 4. IR spectrum of **3a** (upper trace) and BChE-**3a** (lower trace) in the  $\nu_{\text{CO}}$  spectral range. See Experimental part for details.

metal coordinated maleimidato ligand is also feasible as in the organic series. The phospho-derivatives obtained from compound **1a** were sufficiently stable to perform some biological tests on the two cholinesterases AChE and BChE.

There is an on-going interest in the design of new inhibitors of cholinesterases because these molecules represent the only class of drugs administered to patients with Alzheimer's disease [27]. Among them, phosphonate derivatives may be of interest because of their stability in water. Because cholinesterases are also the target for certain agrochemicals (insecticides) and nerve agents, they have stimulated numerous studies. Therefore, the active site of AChE and BChE is now well known thanks to a wealth of X-ray crystallographic data. It consists of a 20 Å length gorge at the bottom of which are located the esterase subsite including the catalytically active residues Ser and His and the anionic subsite that accommodates the cationic part of the substrate. Aminoacids composition of this latter site differs between AChE and BChE [28], allowing BChE to catalyze the hydrolysis of larger substrates such as butyrylcholine. The gorge of AChE is lined with 14 aromatic residues while 6 of these residues are aliphatic in the case of BChE, making the volume of the gorge 200 Å<sup>3</sup> larger for the latter protein [29]. Both enzymes also display a peripheral anionic site at the entrance of the gorge where ligands such as propidium bind.

On the other hand, several research groups have recently reported very interesting results regarding organometallic enzyme inhibitors for which the transition metal either suitably organizes the ligand in the three-dimensional space [30] or brings an additional reactivity [31]. In this area, several polypyridyl Ru(II) complexes were shown to behave as potent inhibitors of AChE with IC<sub>50</sub> in the submicromolar range [32].

The kinetics assays performed with the new phosphonate diesters **2a** and **3a** and the phosphonic acid **4** gave rather unexpected results. The phosphonic acid behaved as a mixed-type inhibitor towards both AChE and BChE with moderate dissociation constants. The complex bound to the free enzymes with more affinity than to the enzyme-substrate complexes. On the other hand, the phosphonate diphenyl ester was a competitive inhibitor of BChE alone. The question now arises about the mode of binding of these complexes to the cholinesterases.

What may be deduced from the kinetics experiments is that the phosphonic acid complex probably binds to the cholinesterases in a manner that differs from that of the diphenyl ester complex. Complex **3a** operates selectivity between AChE and BChE while complex **4** behaves in a very similar manner towards both enzymes. We may hypothesize that the latter compound does not penetrate very deeply within the enzymes' active site as the main difference between both enzymes from a steric point of view lies in the wideness of the gorge and the substrate binding site. Conversely, complex **3a** likely occupies BChE's active site. Furthermore, the phenoxy groups seem to play a role in the binding of **3a** to BChE as **2a** bound neither to AChE nor to BChE. The inability of the diphenyl ester complex to bind to AChE may also be related to steric reasons, as the size of this complex may be too large with respect to the diameter of the gorge that is much narrower in the case of AChE.

Given the fact that **3a** likely binds to the esterase subsite of BChE's active site and possesses two phenoxy leaving groups, it was not unexpected that this compound should be able to phosphorylate the catalytically active serine residue. Indeed, **3a** was shown to slowly and almost fully inactivate BChE. Furthermore as this inactivation was partly reversible in the long term and reactivation was accelerated by addition of the strong nucleophile pralidoxime, it is highly probable that inhibition occurred through enzyme phosphorylation. Conversely, the inability of the complex to bind to AChE probably forbade inactivation to take place.

#### 4. Conclusions

The phospho-Michael addition of anions of dialkylphosphites to the double bond of the maleimidato ligand coordinated to several transition metals successfully yielded phosphonate diester derivatives that were characterized by classical spectroscopic means including X-ray crystallography. The dimethyl phosphonate ester of the iron compound was converted into the phosphonic acid via transesterification with TMSBr. Biochemical activity studies of the iron derivatives revealed an interesting behavior of these complexes vis-à-vis certain serine hydrolases. While the dimethyl derivative had no effect on AChE and BChE, the diphenyl adduct

selectively inhibited BChE in a competitive fashion and the phosphonic acid complex inhibited both AChE and BChE in a mixed-type fashion. Furthermore, the diphenyl ester complex inactivated both BChE and chymotrypsin (and not AChE) in a time-dependent fashion with rates depending on the enzyme. Further studies carried out with BChE revealed that inactivation occurred via phosphorylation of the catalytically active serine residue, thus providing an original way to site-selectively label these enzymes with a metallocarbonyl moiety.

## 5. Experimental

### 5.1. General remarks

NMR spectra were recorded in CDCl<sub>3</sub>, CD<sub>3</sub>OH and D<sub>2</sub>O on VARIAN GEMINI 200BB (200 MHz for <sup>1</sup>H, <sup>31</sup>P and <sup>13</sup>C) and AVANCE TM DRX500 (500 MHz for <sup>1</sup>H) spectrometers and referenced to internal TMS. IR spectra were recorded as KBr pellets on a FT-IR NEXUS (Thermo Nicolet) spectrometer. All solvents were purified according to standard procedures. Chromatographic separations were performed on Silica gel Merck 60 (230–400 mesh ASTM). All reactions were carried out under argon.

### 5.2. Materials

Complexes **1a–c** were synthesized according to literature procedures [4,5]. 1,8-diazabicyclo-(5,4,0)undec-7-ene (DBU) was purchased from Aldrich. Acetylthiocholine (ATCh), acetylcholinesterase (AChE) from electrical eel, type VI-S (EC 3.1.1.7) and  $\alpha$ -chymotrypsin (CT) from bovine pancreas type II (EC 3.4.21.1) were obtained from Sigma. Tetramethylsilyl bromide (TMSBr), dimethylphosphite diphenylphosphite butyrylcholinesterase (BChE) from horse serum (EC 3.1.1.8) and butyrylthiocholine iodide (BTCh) were obtained from Fluka. Suc-Ala-Ala-Ala-Pro-Phe-pNA (Suc-AAPFPNa) was obtained from Bachem. 5,5'-Dithiobis(2-nitrobenzoic acid) (DTNB) was obtained from Lancaster. Pralidoxime was obtained from Acros.

### 5.3. Syntheses

#### 5.3.1. Metallocarbonyl dimethyl phosphonate complexes **2a–c**

An argon-saturated solution of metallocarbonyl complex **1a–c** (0.18 mmol) in dichloromethane was treated with dimethylphosphite (33  $\mu$ l, 0.36 mmol) containing DBU (27 mg, 0.18 mmol). The reaction mixture was stirred overnight at room temperature. The mixture was purified by column chromatography. A yellow band containing a small amount of the substrates **1a–c** was eluted with chloroform, followed by second band (yellow for **2a** and orange for **2b–c**) of product eluted with chloroform-methanol 4:1 for **2a** and CH<sub>2</sub>Cl<sub>2</sub>/ethyl acetate 3:1 for **2b–c**. Crystallization from diethyl ether/heptane (3:1) afforded analytically pure samples **2a–b**.

**2a:** Yield 48.6 mg (69%) <sup>1</sup>H NMR (CDCl<sub>3</sub>,  $\delta$  in ppm): 2.7–3.35 (m, 3H, succinimide), 3.84 (d,  $J$  = 11 Hz, 3H, OCH<sub>3</sub>), 3.78 (d,  $J$  = 12.8 Hz, 3H, OCH<sub>3</sub>), 5.04 (s, 5H, Cp). <sup>13</sup>C NMR (CDCl<sub>3</sub>,  $\delta$  in ppm): 33.6 (d,  $J_{CP}$  = 3.7 Hz), 42.0 (d,  $J_{CP}$  = 140.5 Hz), 52.9 (d,  $J_{CP}$  = 6.9 Hz), 53.8 (d,  $J_{CP}$  = 6.7 Hz), 85.09 (s, Cp), 184.1 (d,  $J_{CP}$  = 6.3 Hz), 187.9 (d,  $J_{CP}$  = 6.1 Hz), 212.0 (s). <sup>31</sup>P NMR (CDCl<sub>3</sub>,  $\delta$  in ppm): 12.57. IR ( $\nu$  in cm<sup>-1</sup>): 2056, 2009 (C=O), 1641 (C=O imide), 1228 (P=O). Anal. Calc. for C<sub>13</sub>H<sub>14</sub>FeNO<sub>7</sub>P C, 40.76; H, 3.68; N, 3.66; found: C, 40.41; H, 3.82; N, 3.85.

**2b:** Yield 65 mg (80%) <sup>1</sup>H NMR (CDCl<sub>3</sub>,  $\delta$  in ppm): 2.9–3.4 (m, 3H, succinimide), 3.87 (d,  $J$  = 12 Hz, 3H, OCH<sub>3</sub>), 3.80 (d,  $J$  = 12 Hz, 3H, OCH<sub>3</sub>), 5.57 (s, 5H, Cp), <sup>31</sup>P NMR (CDCl<sub>3</sub>,  $\delta$  in ppm): 21.89. IR ( $\nu$  in cm<sup>-1</sup>): 2054, 1977 (C=O), 1651 (C=O imide), 1288 (P=O). Anal. Calc. for C<sub>14</sub>H<sub>14</sub>MoNO<sub>8</sub>P C, 37.27; H, 3.13; N, 3.1; found: C, 37.41; H, 3.58; N, 3.49.

**2c:** Yield 72 mg (75%), <sup>1</sup>H NMR (CDCl<sub>3</sub>,  $\delta$  in ppm): 2.7–3.5 (m, 3H, succinimide), 3.79 (d,  $J$  = 12 Hz, 3H, OCH<sub>3</sub>), 3.88 (d,  $J$  = 12 Hz, 3H, OCH<sub>3</sub>), 5.68 (s, 5H, Cp) <sup>31</sup>P NMR (CDCl<sub>3</sub>,  $\delta$  in ppm): 23.46. IR (KBr) (cm<sup>-1</sup>): 2046, 1959, (C=O), 1659 (C=O imide), 1319 (P=O). Anal. Calc. for C<sub>14</sub>H<sub>14</sub>NO<sub>8</sub>PW C, 31.19; H, 2.62; N, 2.6; found: C, 31.08; H, 2.91; N, 2.87.

#### 5.3.2. Metallocarbonyl diphenyl phosphonate complex **3a**

An argon-saturated solution of metallocarbonyl complex **1a** (49 mg, 0.18 mmol) in dichloromethane was treated with diphenylphosphite (55.7  $\mu$ l, 0.36 mmol) containing DBU (27 mg, 0.18 mmol). The reaction mixture was stirred 48 h at room temperature. The mixture was purified by column chromatography. A yellow band containing a small amount of substrate **1a** was eluted with chloroform, followed by a second yellow band of product eluted with ethyl acetate/chloroform 1:3. Crystallization from diethyl ether/heptane (3:1) afforded analytically pure sample **3a**. Yield 49.5 mg (54%). <sup>1</sup>H NMR (CDCl<sub>3</sub>,  $\delta$  in ppm): 2.95–3.2 (m, 2H, CH<sub>2</sub>), 3.5–3.7 (m, H, CH), 5.03 (s, 5H, Cp), 7.15–7.35 (m, 10H). <sup>31</sup>P NMR (CDCl<sub>3</sub>,  $\delta$  in ppm): 15.87. IR ( $\nu$  in cm<sup>-1</sup>): 2039, 1994 (C=O), 1648 (C=O imide), 1274 (P=O). Anal. Calc. for C<sub>23</sub>H<sub>18</sub>FeNO<sub>7</sub>P C, 54.46; H, 3.58; N, 2.76; found: C, 54.19; H, 3.32; N, 2.49.

#### 5.3.3. Phosphonic acid **4**

TMSBr (25  $\mu$ l, 0.188 mmol) was added to a solution of **2a** (36 mg, 0.094 mmol) in dry dichloromethane (2 ml). After 1 h at r.t., excess TMSBr was removed by rotary evaporation and MeOH was added and stirred for 1 h. After evaporation of solvent, compound **4** was obtained as an orange oil. Yield 15 mg (45.5%). <sup>1</sup>H NMR (CD<sub>3</sub>OH,  $\delta$  in ppm): 2.8–3.5 (m, 3H, succinimide), 5.22 (s, 5H, Cp). <sup>31</sup>P NMR (D<sub>2</sub>O,  $\delta$  in ppm): 15.86. IR ( $\nu$  in cm<sup>-1</sup>): 2051, 2002 (C=O), 1589 (C=O imide), 1186 (P=O). FAB MS  $m/e$  = 356 (M+H)<sup>+</sup>.

#### 5.4. X-ray structural determination of **2a**

Crystals of **2a** were obtained from a diethyl ether and heptane solution of complex. Single crystals suitable for X-ray measurement were mounted on glass-fibres. X-ray diffraction data were collected at 293 K on Rigaku AFC5S four-circle diffractometer using Mo K $\alpha$  radiation. The unit cells were determined from 25 reflections. The structure was solved by direct methods using SHELXS-97 [33] and refined by full-matrix least square method on  $F^2$  using SHELXL-97 [34]. After the refinement with isotropic displacement parameters, refinement was continued with anisotropic displacement parameters for all non-hydrogen atoms. All hydrogen atoms were placed on geometrically idealized positions and constrained to ride on their parent atoms, with a C–H distance of 0.950 Å and  $U_{iso}(H) = 1.2U_{eq}(C)$ . The molecular geometry was calculated by PARST97 [35] and PLATON [36]. Fig. 1 has been prepared using PLATON [36]. Table 2 contains selected geometrical parameters.

### 5.5. Enzyme assays

#### 5.5.1. Butyrylcholinesterase

Activity measurements were performed on the basis of the Ellman's thiol assay according to Doctor [37] with slight modification. A stock solution of BChE (10 mg/ml) was prepared in 50 mM phosphate buffer pH 8.0. The solution was diluted to 20  $\mu$ g/ml in the same buffer and 10  $\mu$ l were dispensed in wells of a microplate (Greiner). The substrate mixture was prepared by mixing BTCh (50 mM in H<sub>2</sub>O, 50  $\mu$ l) and DTNB (1 mM in 100 mM Tris–HCl, 0.01% gelatine pH 7.6, 5 ml) and incubated at 30 °C. The enzymatic reaction was initiated by dispensing the substrate mixture into the wells (200  $\mu$ l). The optical density at 415 nm was monitored dur-

ing 4 min with a microplate reader (model 680, Biorad) thermostated at 30 °C. In these conditions, BChE has a specific activity of 6 u/mg of solid).

### 5.5.2. Acetylcholinesterase

Activity measurements were performed as above except that BTCh was replaced by ATCh and the enzyme solution was diluted to 0.8 µg/ml. In these conditions, AChE has a specific activity of 166 u/mg of protein.

### 5.5.3. Chymotrypsin

Activity measurements were performed according to the assay described by DelMar et al. [38] transposed to a microplate format. A 1 mM stock solution of SucAAPFPNa was prepared in DMSO. The working solution was prepared by diluting 1 part of stock solution with 8 parts of 50 mM Tris–HCl, 20 mM CaCl<sub>2</sub> pH 7.6. A stock solution of CT was prepared in 1 mM HCl (10 mg/ml, kept at –20 °C for no more than one week). Immediately before the assay, the enzyme was diluted to 20 µg/ml in 1 mM HCl and 20 µl were dispensed into wells of a microplate. The enzymatic reaction was initiated by addition of substrate (180 µl). The optical density at 415 nm was monitored during 2 min with a microplate reader. In these conditions, CT has a specific activity of 68 ± 2 u/mg of solid.

### 5.6. Reversible inhibition assays

AChE (0.78 µg/ml in 50 mM phosphate buffer pH 8.0, 10 µl) was mixed with MeOH (20 µl) or inhibitor (10 mM in MeOH, 20 µl) and a mixture of ATCh (0.1–0.5 mM) and 1 mM DTNB (200 µl). The optical density was monitored at 415 nm during 4 min at 30 °C. The same procedure was applied with BChE using an enzyme solution of 20 µg/ml and a substrate concentration range of 0.05–0.3 mM. The interaction between the enzymes and the inhibitors can be described by Scheme 4 where E is the enzyme, S in the substrate, I is the inhibitor, ES is the enzyme–substrate complex and P<sub>1</sub> and P<sub>2</sub> are the products. K<sub>i</sub> and K'<sub>i</sub> are the inhibition constants reflecting the interaction of inhibitor with free enzyme and enzyme–substrate complex, respectively.

The Michaelis–Menten equation reflecting both interactions is:

$$v = \frac{v_{\max} \times [S]}{\alpha \times K_M + \alpha' \times [S]} = \frac{(1/\alpha') \times v_{\max} \times [S]}{(\alpha/\alpha') \times K_M + [S]}$$

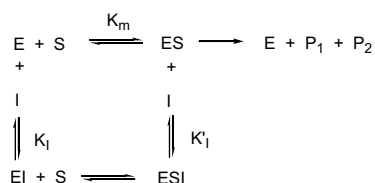
where the modifying factors  $\alpha$  and  $\alpha'$  are:

$$\alpha = 1 + \frac{[I]}{K_i} \quad \text{and} \quad \alpha' = 1 + \frac{[I]}{K'_i}$$

K<sub>M</sub>, v<sub>max</sub>, (1/α')v<sub>max</sub> and (α/α')K<sub>M</sub> were estimated by non linear regression analysis of rate versus substrate concentration plots in the absence or presence of inhibitor with Kaleidagraph.

### 5.7. Measurement of IC<sub>50</sub>

BChE (100 µg/ml, 90 µl) was mixed with **3a** (0–20 mM, 10 µl) in wells of a microtiter plate. After 1 h, the mixtures (10 µl) were



**Scheme 4.** Reversible inhibition. Competitive type: K'<sub>i</sub> = 0; Mixed type: K<sub>i</sub> ≠ K'<sub>i</sub>; Non-competitive type: K<sub>i</sub> = K'<sub>i</sub>.

transferred into adjoining wells. A mixture of substrate (0.5 mM) and DTNB (1 mM) in 100 mM Tris–HCl pH 7.6 (200 µl) was added to the wells and the optical density was immediately monitored at 415 nm during 4 min at 30 °C. The IC<sub>50</sub> was calculated from linear regression of plot of logit(% residual activity) versus log([**3a**]) (logit(% residual activity) = log(% residual activity)/(100 – % residual activity)).

### 5.8. Time-dependent inactivation of AChE and BChE

BChE (10 mg/ml in 50 mM phosphate buffer pH 8, 5 µl) was mixed with 50 mM Tris–HCl buffer pH 7.6 (175 µl) and inhibitor (10 mM in MeOH, 20 µl). A control experiment was performed where the complex solution was replaced by MeOH. Aliquots (2 µl) were withdrawn at recorded times, diluted to the tenth and the enzymatic activity was measured under standard conditions (see above). The logarithm of the % residual activity was plotted as a function of time to deduce the pseudo-first order rate constant k<sub>obs</sub>. The same procedure was applied with AChE (0.178 mg/ml).

### 5.9. Time-dependent inactivation of CT

CT (10 mg/ml in 1 mM HCl, 100 µl) was mixed with 50 mM Tris–HCl buffer pH 7.6 (350 µl) and **3a** (10 mM in MeOH, 50 µl). A control experiment was performed for which **3a** was replaced by MeOH. Aliquots (2 µl) were withdrawn at recorded times, diluted to 20 µg/ml and the enzymatic activity was measured under standard conditions (see above). The logarithm of the % residual activity was plotted as a function of time to deduce the pseudo-first order rate constant k<sub>obs</sub>.

### 5.10. Reactivation studies

BChE (10 mg/ml in 50 mM phosphate buffer pH 8, 5 µl) was mixed with 50 mM Tris–HCl buffer pH 7.6 (185 µl) and **3a** (20 mM in MeOH, 10 µl). The mixture was incubated overnight at room temperature then submitted to gel filtration to eliminate excess complex (5 ml bed volume D-salt column, Pierce chemicals) using the same Tris buffer as eluent. One half of the protein solution collected (0.25 ml) was allowed to stand at room temperature and aliquots (10 µl) were removed at specified times and the enzymatic activity determined as above. Pralidoxime was added to the second half of the solution of blocked BChE (final concentration 2 mM). After 15 h, the residual enzymatic activity was measured on a 10-µl aliquot and corrected by spontaneous hydrolysis of BTCh in the presence of pralidoxime. The reactivation rate R was calculated according to [39] from the following equation:

$$R = \left( 1 - \frac{v_0 - v_R}{v_0 v_i} \right) \times 100,$$

where v<sub>0</sub> is the substrate hydrolysis rate by intact BChE, v<sub>R</sub> is the hydrolysis rate by reactivated BChE and v<sub>i</sub> is the hydrolysis rate by inhibited BChE.

### 5.11. IR analysis of BChE **3a**

BChE (10 mg/ml in 50 mM phosphate buffer pH 8, 50 µl) was mixed with 50 mM Tris–HCl buffer pH 7.6 (130 µl) and **3a** (10 mM in MeOH, 20 µl). The mixture was incubated in the dark overnight and submitted to gel filtration to eliminate excess complex (5 ml bed volume Econopac P6 column, Biorad) using 0.15 M NaCl as eluent. The protein solution was concentrated with a centrifugal filter (Ultrafree 0.5, 10 K NMWL, Millipore). The resulting solution (10 µl) was deposited on a 6 mm diameter nitrocellulose membrane

(Transfer blot, Biorad). The IR spectrum of the dry membrane was recorded with an FT- spectrometer (Tensor 27, Bruker) and the absorbance of a blank membrane was manually subtracted.

### Acknowledgements

The French Ministry of Foreign Affairs and the Polish Ministry of Science and Education are gratefully acknowledged for scientific exchanges through the “POLONIUM” programme.

### Appendix A. Supplementary material

CCDC 701469 contains the supplementary crystallographic data for this paper. These data can be obtained free of charge from The Cambridge Crystallographic Data Centre via [www.ccdc.cam.ac.uk/data\\_request/cif](http://www.ccdc.cam.ac.uk/data_request/cif). Supplementary data associated with this article can be found, in the online version, at [doi:10.1016/j.jorganchem.2008.10.057](https://doi.org/10.1016/j.jorganchem.2008.10.057).

### References

- [1] T.L. Schull, D.A. Knight, *Coord. Chem. Rev.* 249 (2005) 1269–1282.
- [2] J. Wu, Y. Song, E. Hang, H. Hou, Y. Fan, Y. Zhou, *Chem. Eur. J.* 12 (2006) 5823–5831.
- [3] K. Moonen, I. Laureyn, C.V. Stevens, *Chem. Rev.* 104 (2004) 6177–6215.
- [4] B. Rudolf, J. Zakrzewski, *Tetrahedron Lett.* 35 (1994) 9611–9612.
- [5] B. Rudolf, M. Palusiak, J. Zakrzewski, M. Salmain, G. Jaouen, *Bioconjugate Chem.* 16 (2005) 1218–1224.
- [6] B. Rudolf, J. Zakrzewski, M. Salmain, G. Jaouen, *New J. Chem.* (1998) 813–818.
- [7] B. Rudolf, J. Zakrzewski, G. Celichowski, M. Salmain, A. Vessières, G. Jaouen, *Appl. Organomet. Chem.* 18 (2004) 105–110.
- [8] N. Fischer-Durand, M. Salmain, B. Rudolf, A. Vessières, J. Zakrzewski, G. Jaouen, *ChemBioChem* 5 (2004) 519–525.
- [9] N. Fischer-Durand, M. Salmain, B. Rudolf, L. Jugé, V. Guérineau, O. Laprèvote, A. Vessières, G. Jaouen, *Macromolecules* 40 (2007) 8568–8575.
- [10] P. Haquette, M. Salmain, K. Svedlung, A. Martel, B. Rudolf, J. Zakrzewski, S. Cordier, T. Roisnel, C. Fosse, G. Jaouen, *ChemBioChem* 8 (2007) 224–231.
- [11] F.H. Allen, C.A. Baalham, J.P.M. Lommerse, P.R. Raithby, *Acta Crystallogr. B* 54 (1998) 320–329.
- [12] K.-S. Law, R.A. Acey, C.R. Smith, D.A. Benton, S. Soroushian, B. Eckenrod, R. Stedman, K.A. Kantardjiev, K. Nakayama, *Biochem. Biophys. Res. Commun.* 355 (2007) 371–378.
- [13] N. Zhang, J.E. Casida, *Bioorg. Med. Chem.* 10 (2002) 1281–1290.
- [14] J.C. Powers, J.L. Asgian, O.D. Ekici, K.E. James, *Chem. Rev.* 102 (2002) 4639–4750.
- [15] J.-F. Cavalier, G. Buono, R. Verger, *Acc. Chem. Res.* 33 (2000) 579–589.
- [16] J. Patočka, K. Kuča, D. Jun, *Acta Med. (Hradec Králové)* 47 (2004) 215–228.
- [17] J.E. Casida, G.B. Quistad, *Chem. Biol. Interact.* 157 (2005) 277–283.
- [18] E.L. Becker, T.R. Fukuto, D.C. Canham, E. Boger, *Biochemistry* 2 (1963) 72–76.
- [19] Q. Zhao, I.M. Kovach, A. Bencsura, A. Papathanassiou, *Biochemistry* 33 (1994) 8128–8138.
- [20] A. Tramontano, B. Ivanov, G. Gololobov, S. Paul, *Appl. Biochem. Biotechnol.* 83 (2000) 233–243.
- [21] C.A. Kruihof, M.A. Casado, G. Guillena, M.R. Egmond, A. van der Kerk-van Hoof, A.J.R. Heck, R.J.M. Klein Gebbink, G. Van Koten, *Chem. Eur. J.* 11 (2005) 6869–6877.
- [22] J. Oleksyszyn, J.C. Powers, *Biochemistry* 30 (1991) 485–493.
- [23] A.N. Davison, *Biochem. J.* 60 (1955) 339–346.
- [24] I.B. Wilson, S. Ginsburg, *Arch. Biochem. Biophys.* 54 (1955) 569–571.
- [25] D. Enders, A. Saint-Dizier, M.-I. Lannou, A. Lenzen, *Eur. J. Inorg. Chem.* (2006) 29–49.
- [26] Z. Jiang, Y. Zhang, W. Ye, C.-H. Tan, *Tetrahedron Lett.* 48 (2007) 51–54.
- [27] A. Martinez, A. Castro, *Expert Opin. Investig. Drug.* 15 (2006) 1–12.
- [28] P. Taylor, Z. Radic, N.A. Hosea, S. Camp, P. Marchot, H.A. Berman, *Toxicol. Lett.* 82/83 (1995) 453–458.
- [29] A. Saxena, A.M.G. Redman, X. Jiang, O. Lockridge, B.P. Doctor, *Biochemistry* 36 (1997) 14642–14651.
- [30] (a) E. Meggers, G.E. Atilla-Gokcumen, H. Bregman, J. Maksimoska, S.P. Mulcahy, N. Pagano, D.S. Williams, *Synlett* (2007) 1177–1189;  
(b) H. Bregman, D.S. Williams, G.E. Atilla, P.J. Carroll, E. Meggers, *J. Am. Chem. Soc.* 126 (2004) 13594–13595;  
(c) G.E. Atilla-Gokcumen, D.S. Williams, H. Bregman, N. Pagano, E. Meggers, *ChemBioChem* 7 (2006) 1443–1450;  
(d) E. Meggers, *Curr. Opin. Chem. Biol.* 11 (2007) 287–292.
- [31] W.H. Ang, A. De Luca, C. Chapuis-Bernasconi, L. Juillerat-Jeanneret, M. Lo Bello, P.J. Dyson, *ChemMedChem* 2 (2007) 1799–1806.
- [32] S.P. Mulcahy, R. Korn, X.L. Xie, E. Meggers, *Inorg. Chem.* 47 (2008) 5030–5032.
- [33] G.M. Sheldrick, *SHELXS*, Program for crystal structure solution, University of Göttingen, Germany, 1997.
- [34] G.M. Sheldrick, *SHELXL*, Program for refinement of crystal structures, University of Göttingen, Germany, 1997.
- [35] M. Nardelli, *J. Appl. Crystallogr.* 29 (1996) 296.
- [36] A.L. Spek, *PLATON – Molecular geometry program*, University of Utrecht, The Netherlands, 1998.
- [37] B.P. Doctor, L. Toker, E. Roth, I. Silman, *Anal. Biochem.* 166 (1987) 399–403.
- [38] E.G. DelMar, C. Largman, J.W. Brodrick, M.C. Geokas, *Anal. Biochem.* 99 (1979) 316–320.
- [39] D. Jun, L. Musilovic, K. Kuca, J. Kassa, J. Bajgar, *Chem. Biol. Interact.* (2008), [doi:10.1016/j.cbi.2008.05.004](https://doi.org/10.1016/j.cbi.2008.05.004).